



Acoustic imaging of surface ship wakes

Alexei KOUZOUBOV¹; Shane WOOD²; Richard ELLEM³

^{1,2,3} Defence Science and Technology Organisation, Australia

ABSTRACT

Techniques for three-dimensional visualization of a surface ship bubbly wake using a high-frequency narrow beam profiling sonar are reported. Instrumentation, experimental set-up, and data processing are described. An Imagenex profiling sonar is mounted on the side of a boat at about 1 m below the water surface. The narrow pencil beam scans the water through the sectors whose plane is perpendicular to the direction of the boat motion. Two scanning techniques were used. In the first, the wake is scanned from the side with about 50° sectors, with the profiling boat moving slowly along the wake in the direction opposite to that of wake laying ship. In the second technique the boat moves inside the wake and scans it with a 180° sector. Both techniques have their advantages and disadvantages which are discussed in the paper. The GPS coordinates of the profiling boat and angular position of the sonar head are recorded. These data allow building a three-dimensional image of the bubbly wake during post-processing.

Keywords: Ship wake, Bubbles, Scattering, Transmission I-INCE Classification of Subjects Number(s): 23.6, 23.9

1. INTRODUCTION

Modelling of surface ship bubbly wakes is of high importance in military applications. This is a very difficult problem and state-of-the-art numerical models of surface ship bubbly wakes still rely on empirical data on bubble generation by breaking bow and stern waves and by propellers or jet propulsors. Even if all elements of the model are well-developed the validation of the whole model of the surface ship wake is still required before the model can be safely used in any further analysis. The wake model validation would require various quantitative data on the wake: geometry of the wake cross-section and its time history, wake turbulence and intermittence, air volume fraction and bubble size distribution in the wake etc. Due to the harsh environment in the turbulent wake of a surface ship any measurements directly in the wake are extremely difficult and almost non-existent. Remote sensing techniques are therefore very attractive as they do not interfere with the flow being measured and the instruments are not subject to a severe turbulent environment. However, the remote sensing instruments do not measure the wake parameters directly but rather its various signatures from which the wake parameters have to be inferred.

There are several above-surface remote sensing methods of obtaining information on the ship wakes. Synthetic Aperture Radar (SAR) has been extensively used for detection and measurement of sea surface roughness damping in the wake centreline (1). Conventional optical methods were used for imaging of ship Kelvin waves and turbulent wake, but those methods were limited to the surface signature of the wake. They provide no information on the wake's underwater parameters. There were attempts to establish a quantitative relationship between bubble concentration in the ship wake and its visual reflectance spectrum, or colour (2). However, this relationship is not accurate enough for reliable solution of the inverse problem. There are also reports indicating that some information on the underwater structure of the ship wake can be obtained using lidars (3).

So far the most popular approach to the ship wakes experimental research is based on using various sonars. The first acoustic measurements of ship wake date back to the 1940's when wakes of various vessels were insonified by sonars with several different frequencies from 15 to 60 kHz. Some

¹ alexei.kouzoubov@dsto.defence.gov.au

² shane.wood@dsto.defence.gov.au

³ richard.ellem@dsto.defence.gov.au

empirical relations for wake geometry and acoustic strength were derived from these experiments (4).

Trevorrow *et al.* (5) investigated surface ship wakes using a set of six upward looking sonars with combined frequency range 28 to 400 kHz, which provided vertical profiles of backscattering strength due to microbubbles. Four steerable sidescan sonars generated two-dimensional images of the wake, which were used to determine location, width, and persistence of ship wakes. Wakes of three vessels were investigated and empirical relationship for wake width and depth versus time were suggested. Some acoustic measurements of the wake of a manoeuvring ship were performed by Trevorrow *et al.* (6) using recording buoys and an acoustic source transmitting Linear Frequency Modulated (LFM) pulses with a frequency range of 2-18 kHz.

Wake measurements using a bottom-mounted upward-looking multibeam Reson 8101 echosounder were performed by Weber *et al.* (7). With a sonar centre frequency of 240 kHz, it has 101 identical beams of angular width $1.5^\circ \times 1.5^\circ$ resulting in 150° sector. The sonar provides images of the wake cross-section. Good angular resolution allowed detecting the wake splitting in two distinct tails.

Acoustic transmission through the bubbly ship wake was measured in a series of experiments by Stanic *et al.* (8,9). The measurements were performed in a range of frequencies, which allowed the authors to infer the bubble size distribution in the wake.

Soloviev *et al.* (10) used a downward-looking sonar mounted on a small boat to insonify a ship's wake while the boat was crossing the wake with a "snakelike" trajectory thus building a three dimensional image of the bubbly wake. Simultaneous images from space-based SAR were also obtained in this experiment. An attempt was made to correlate between the SAR and sonar data.

Increasing capability in sonar technology allows investigation of ship wakes in more detail. Thus Soloviev *et al.* (11) used a 3D sonar imaging system, CodaOctopus Echoscope, to produce high-resolution 3D images of ship wakes, which are important for the validation of hydrodynamic models of the wakes but are also very expensive.

In this document we report the results of a test of using a relatively inexpensive narrow beam profiling sonar from Imagenex (12) for obtaining three-dimensional images of ship wakes.

2. EXPERIMENT SET-UP

In this research we used an Imagenex model 881L digital multi-frequency profiling sonar (12). The sonar transducer and electronics are housed in a relatively small cylinder of approximately 230 mm long and 80 mm diameter. The sonar operating frequency is tuneable from 280 kHz to 1.1 MHz in steps of 5 kHz. It uses a pencil shaped beam, the width of which depends on the selected frequency. According to the sonar specifications the beam width is 1.4° at 1 MHz, 2.1° at 675 kHz, and 2.4° at 600 kHz (12). Range scale can be selected from 1 m up to 100 m. Range resolution is 2 mm for range scales 1 to 4 m, and 10 mm for range scales of 5 m and up. There are five scanning speeds with the step size varying from 0.3° for slowest to 2.4° for fastest scanning speed. The beam can be scanned in side scan, polar, and sector modes. The data resolution is 8-bit.

It is important to select an optimum frequency for profiling of the bubbly ship wakes. The strongest response to the acoustic pulse comes from the bubbles of resonant size for given sonar frequency. Thus the radius of the resonant bubble is $12\text{ }\mu\text{m}$ at 300 kHz, and $6\text{ }\mu\text{m}$ at the frequency of 600 kHz. Although at higher frequency the sonar beam is narrower providing a better resolution and clearer image of solid objects, there are not many very small bubbles in a typical wake and the bubble cloud is more transparent to the sound of higher frequency. The sonar has been calibrated using a stainless steel sphere of 100 mm diameter at different frequencies. Analyzing sonar returns from the sphere we arrived at the conclusion that 450 kHz is the most suitable frequency for imaging the bubbly wakes being the lowest frequency in the sonar range with the sufficiently high sensitivity and weakest beam sidelobes.

Two variants of the wake insonification were used in the experiments. They are sketched in Figure 1 and Figure 2. In both cases the sonar head is positioned on a pole deployed over the side of a Rigid-Hulled Inflatable Boat (RHIB) at about 1 m below the water surface. In set-up 1 (Figure 1) the boat is positioned outside the wake and the sonar insonifies the wake in a vertical scanning sector thus producing an acoustic image of the wake slice. With the RHIB moving along the wake a 3D image of the wake can be built.

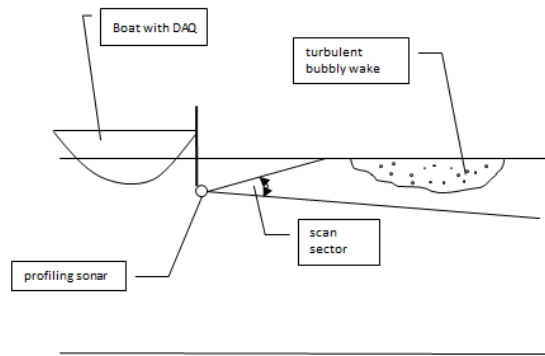


Figure 1. Illustration of the wake insonification set-up 1.

In set-up 2 (Figure 2) the boat is positioned inside the wake with the sonar head located approximately at the centre-line of the wake. The wake is insonified using a scanning sector of more than 180° or even in polar mode, in which case the sonar beam sweeps through the full circle around the sonar head. Again, one scan gives an image of the wake slice and the 3D image is built up increasingly as the boat moves along the wake.

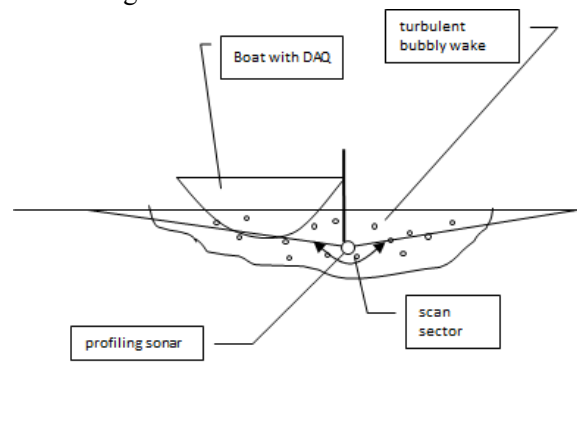


Figure 2. Illustration of the wake insonification set-up 2.

Both of these set-ups have their advantages and disadvantages. Set-up 1 provides less interference with the wake and the positioning of the boat is easier than in set-up 2. Set-up 2 requires manoeuvring the boat into the wake as soon as possible after the passing of the wake-laying ship, which is not always safe to do. The disadvantage of set-up 1 is that due to attenuation and scattering of sound in the wake, the image of the far side of the wake may be distorted especially by the strong wakes of larger ships. A correction for the beam attenuation is required in this case, however, this is not trivial to do.

3. Data coordinate transformation

To form a three-dimensional image of the wake we need to transform sonar data to a fixed coordinate system (x, y, z) with the origin at a point (x_0, y_0, z_0) . The data in the sonar beam are described by the range and the angle of the beam within a plane orthogonal to the sonar head. Within this plane the coordinates of the data bin are designated as (y_i, z_i) . The position of the sonar head itself is defined by its spatial coordinates (x_h, y_h, z_h) and three orientation angles: yaw, pitch, and roll: (α, β, γ) . The coordinates (x_h, y_h) are defined by GPS coordinates of the boat. The vertical coordinate of the sonar head, z_h , is the sonar head depth. It can be affected by the wave action, but because it cannot be measured accurately in real time it is assumed to be constant as measured at the beginning of the experiment. The orientation angles of the sonar head are logged with the frequency of 2 Hz by a directional sensor fixed to the sonar. During the post-processing stage the sonar data is transformed to the fixed coordinate system as follows:

$$\begin{pmatrix} x \\ y \\ z \end{pmatrix} = R(\alpha, \beta, \gamma) \begin{pmatrix} 0 \\ y_i \\ z_i \end{pmatrix} + \begin{pmatrix} x_h - x_0 \\ y_h - y_0 \\ z_h - z_0 \end{pmatrix}$$

where the transformation matrix due to the head rotation is

$$R(\alpha, \beta, \gamma) = R_x(\gamma)R_y(\beta)R_z(\alpha)$$

where

$$R_x(\gamma) = \begin{bmatrix} 1 & 0 & 0 \\ 0 & \cos \gamma & -\sin \gamma \\ 0 & \sin \gamma & \cos \gamma \end{bmatrix}, \quad R_y(\beta) = \begin{bmatrix} \cos \beta & 0 & \sin \beta \\ 0 & 1 & 0 \\ -\sin \beta & 0 & \cos \beta \end{bmatrix}, \quad R_z(\alpha) = \begin{bmatrix} \cos \alpha & -\sin \alpha & 0 \\ \sin \alpha & \cos \alpha & 0 \\ 0 & 0 & 1 \end{bmatrix}$$

4. Data collection

The data presented here were collected in two different experiments. The first experiment took place on 17 February 2014 in the Port River near Adelaide. The wakes of a speed boat and the MV Dolphin Explorer were used to acquire the data. The main parameters of the MV Dolphin Explorer are: length is 34.95 m, beam is 12.8 m, and draft is 1.8 m (13). The GPS coordinates of the wake laying boats were not recorded in this experiment. Sheltered conditions of the Port River resulted in smooth sea surface during the experiment and easy visual detection of the bubbly wakes. The second experiment took place in the outer channel of the Adelaide Port on 12 May 2014. The depth of the channel in the place of the experiment is about 15 m. A dedicated wake laying ship was used for this experiment and its GPS data were logged. The wake laying ship in this experiment was the Research Vessel Ngerin of the South Australian Research and Development Institute (SARDI) (14). The main parameters of the Research Vessel Ngerin are: length is 25 m, beam is 7.2 m, and draft is 3 m. In total eleven runs were executed with different techniques used by the RHIB for acquiring wake data. In all runs the wake laying ship was travelling with a constant speed of 8 knots in an approximately straight course with only a slight turn following the course of the channel.

5. Results

We present data in this report in two forms: raw sonar data and the backscattering cross-section per unit volume. The raw sonar data have the range from 0 to 127 due to 8-bit resolution of A/D converter. The sonar calibration was performed using echoes from a stainless steel sphere of 100 mm diameter. Approximating the target strength of the sphere by that of the rigid sphere we have

$$TS_{sph} = 10 \log_{10} \frac{R_{sph}^2}{4} = -32 \text{ dB for the sphere radius } R_{sph} = 50 \text{ mm}.$$

From this we obtain the sonar calibration constant:

$$K = TS_{sph} - 20 \log_{10} S_{sph} + TVG_{sph} - TL_{sph}$$

where S_{sph} is the raw sonar return from the calibration sphere, TVG_{sph} is the sonar gain at the calibration, TL_{sph} is the two-way transmission loss between sonar and the calibration sphere. The sonar gain combines the constant and time varying parts:

$$TVG = G + 40 \log_{10} r + 2\alpha_s r$$

where G is the constant gain for the sonar in dB, r is the range from sonar in metres, α_s is the sonar setting for sound attenuation in dB/m. The second term in the right-hand side of the above equation is compensation for spherical spreading of the sonar signal, the third term of the time varying gain is the compensation for the attenuation of sound by water. The two-way propagation loss is due to

spherical spreading of the sound energy and its attenuation in water:

$$TL = 40 \log_{10} r + 2\alpha r$$

For calibration, the range r in the above equations is the distance between the sonar head and the calibration sphere.

The sonar data acquired from the wakes are converted from raw sonar data, S , to the volumetric scattering strength S_v measured in dB as follows (15):

$$S_v = 20 \log_{10} S - TVG + K + TL - 10 \log_{10} V$$

where V is the volume insonified by the sonar pulse of length τ :

$$V = \frac{1}{3} \pi \tan^2 \left(\frac{\gamma}{2} \right) \left\{ \left(r + \frac{1}{4} c \tau \right)^3 - \left(r - \frac{1}{4} c \tau \right)^3 \right\}$$

where c is the speed of sound in water, γ is the pencil beam angle.

5.1 Results from experiment set-up 1

Examples of raw sonar data without geometrical correction for the sonar head orientation are presented in Figure 3. All three plots in this figure show the data taken from the MV Dolphin Explorer wake. The wake was scanned from outside using a sector scan of 51° with the sector axis directed horizontally (experimental set-up 1, Figure 1). The sector apex is 1 metre below the water surface. The z-axis is positive in upward direction with zero at the sonar head position. One can see that the image of the wake extends above water surface due to reflections of the sonar beam from water-air interface. The normal practice is to cut the image at the water surface to show only the underwater part of the wake. Here, however, the data are not yet corrected for the sonar head pitch and roll and, therefore, the sea surface is not defined. The left plot in Figure 3 is taken while the RHIB was passing the MV Dolphin Explorer. One can clearly see the reflections from the bow wave and the hull of the wake-laying boat. The centre plot shows the data taken soon after passing the stern of the wake-laying boat. The wake is still dense and narrow here. The middle spot in the wake image is probably associated with the propeller wake. The right plot represents the data from the wake further downstream, where the wake is already weaker and separated in two parts with the propeller wake still present in the middle.

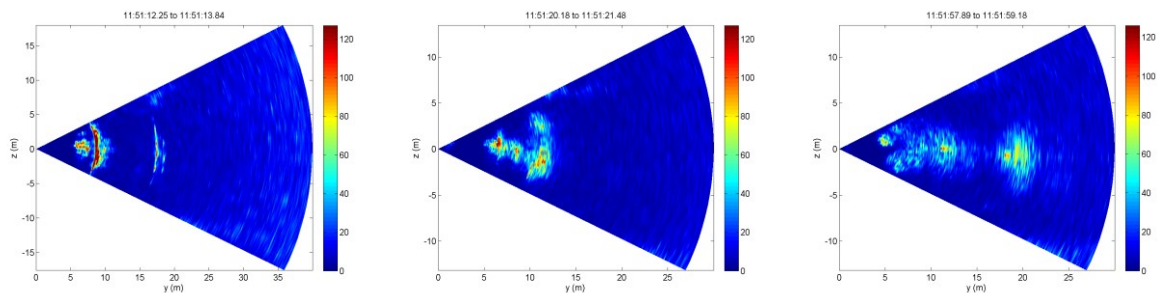


Figure 3. Raw sonar data for MV Dolphin Explorer wake.

Figure 4 illustrates the geometrical correction of the data. It shows the data from the left plot of Figure 3 transferred to the fixed coordinate system and with the above water part of the data removed. The green line in the plot corresponds to the RHIB track. The sonar data are shown in actual beams and range bins without interpolation between the data points as was done in the plots of Figure 3.

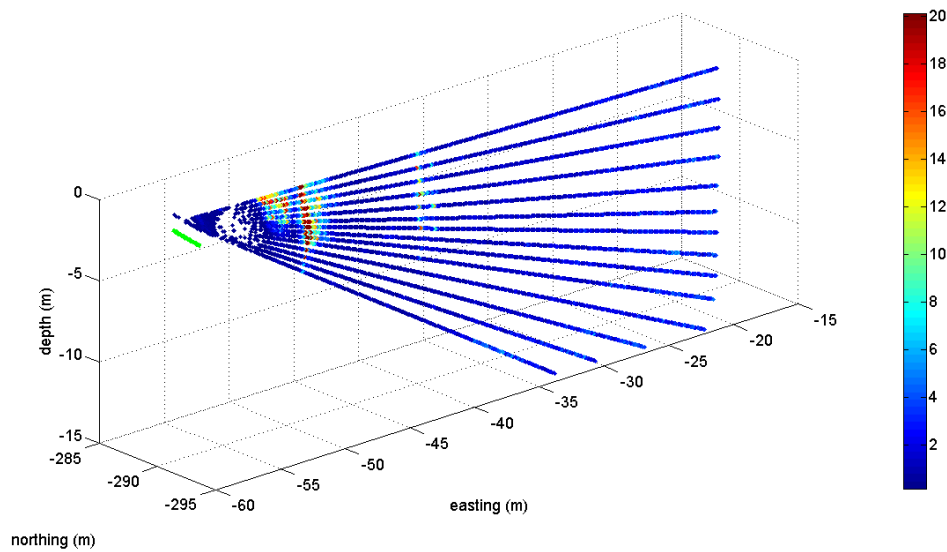


Figure 4. One-scan data geometrically corrected for sonar head orientation and boat motion.

Similar representation of the data is shown in Figure 5 for the whole wake. This time a threshold was applied to the data with the intent to show only sonar returns from the bubbly wake. Certainly, some noise was not completely removed from the data by thresholding as seen at the start of the wake. Here it was probably caused by the multiple strong reflections from the wake-laying boat hull. From the shape of the wake it can be concluded that the boat was making a slight turn. This, however, cannot be verified since the GPS data was not logged for the wake-laying ship. It can also be noted from the plot that the acoustic returns from the wake part further from the RHIB are weaker. This is probably caused by the attenuation of sonar beam in the bubbly wake, for which the data were not corrected. Such a correction is not a trivial procedure, especially for the single frequency sonar data, and was not conducted in this research.

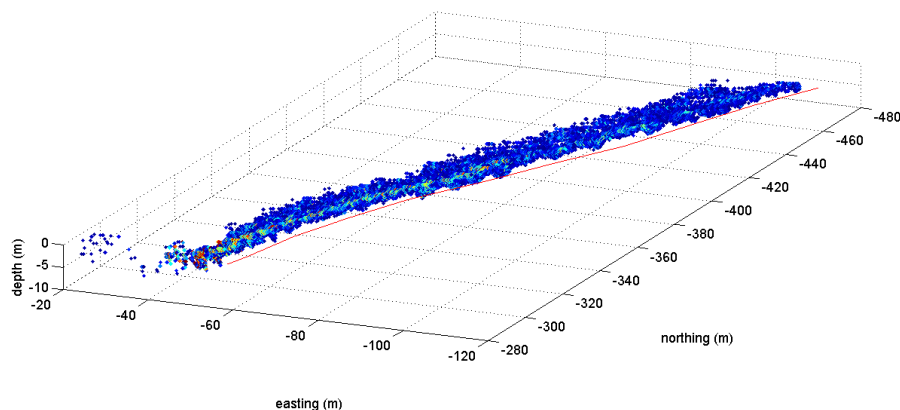


Figure 5. Sonar data bins in the fixed coordinate system. MV Dolphin Explorer wake.

Another form of presentation of three-dimensional images of the wake is shown in Figure 6, which shows isosurface of the raw sonar data at the level of 0.25 of the data maximum value. A characteristic split of the wake in two strips is clearly visible in the plot. To build the wake isosurface the data were interpolated onto a fine rectangular mesh covering the region encompassing the wake.

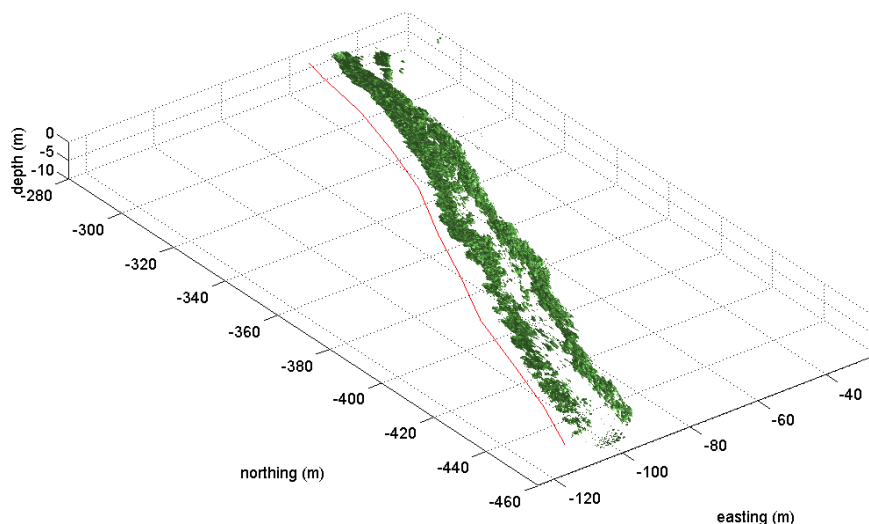


Figure 6. Isosurface of sonar data of MV Dolphin Explorer wake transformed to the fixed coordinate system.

Another example of a three-dimensional image of the wake obtained using the experiment set-up 1 is shown in Figure 7. The data in this figure is obtained from experiments with Ngerin as the wake-laying ship. The figure shows contour slices of the backscattering cross-section per unit volume. Again, the characteristic split tail shape of the wake is apparent from the plot. The plot also displays the track of the RHIB (red line) and the track of Ngerin (black line). The GPS receiver on Ngerin was fitted at starboard edge of the ship's beam, which explains the track position at the edge of the wake. The left branch of the wake in this plot has stronger backscattering cross-section per unit volume. This is due to the reason already mentioned above: sound attenuation in the bubbly wake. Because of this, the part of the wake positioned further from sonar is insonified with weaker sound and backscattered sound is further attenuated on its way back to the receiver.

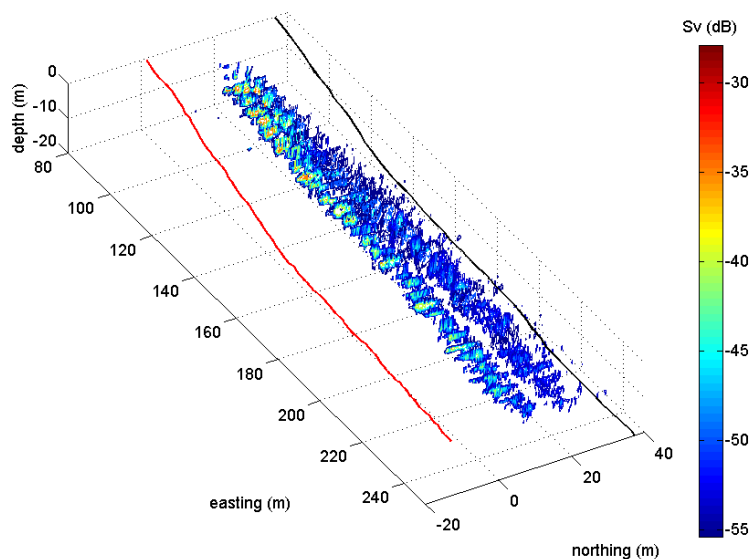


Figure 7. Contour slices of the backscattering cross-section per unit volume of Ngerin wake during run 5. Red line is RHIB track, black line is Ngerin track.

5.2 Results from experiment set-up 2

This section presents results obtained from Ngerin's wake using the experiment set-up 2, in which the wake is insonified from approximately its centreline in wide ($>180^\circ$) sector. Example of one sector

scan of sonar data obtained from Ngerin's wake is presented in Figure 8. The left plot shows the raw sonar data. In the right plot the raw sonar data were converted to the backscattering cross-section per unit volume as described above. One can see that the image of the wake is more symmetrical in scattering strength here than in set-up 1. It does not mean, however, that the wake image is not affected by the beam attenuation. But if sonar is positioned at the centreline of the wake, the attenuation is approximately equal on both sides of the wake. Ideally, the image still should be corrected for acoustic attenuation of the sonar beam in the bubbly wake. This might be addressed in future work.

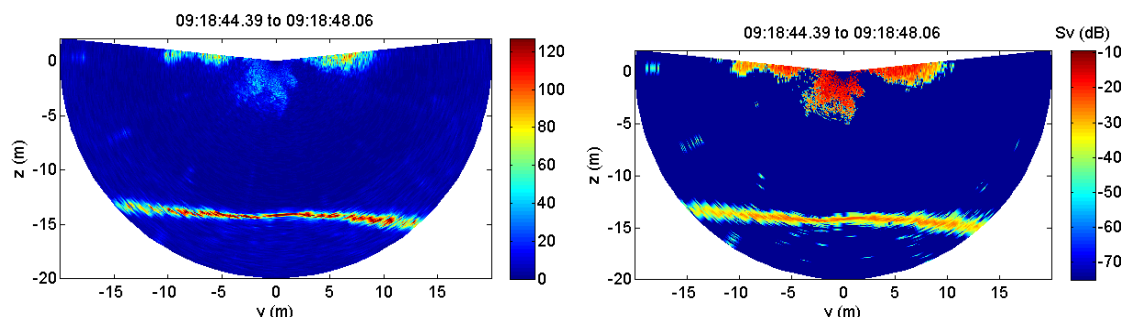


Figure 8. Example of sonar data obtained from Ngerin wake using the experiment set-up 2. Left plot: raw sonar data, right plot: backscattering cross-section per unit volume.

The sector size in the experiment set-up 2 is 189° . Even with the fastest scanning speed, it takes more than 3.5 seconds to complete the scan as can be seen from the titles of the plots in Figure 8. During this time, the RHIB, which is moving at about 3 knots, travels about 6 metres, so the wake in the set-up 2 has less dense sounding than in the set-up 1. The three-dimensional presentation of the scanning sector from Figure 8 is shown in Figure 9. The data here are geometrically corrected for the sonar head orientation. The green line shows the RHIB track.

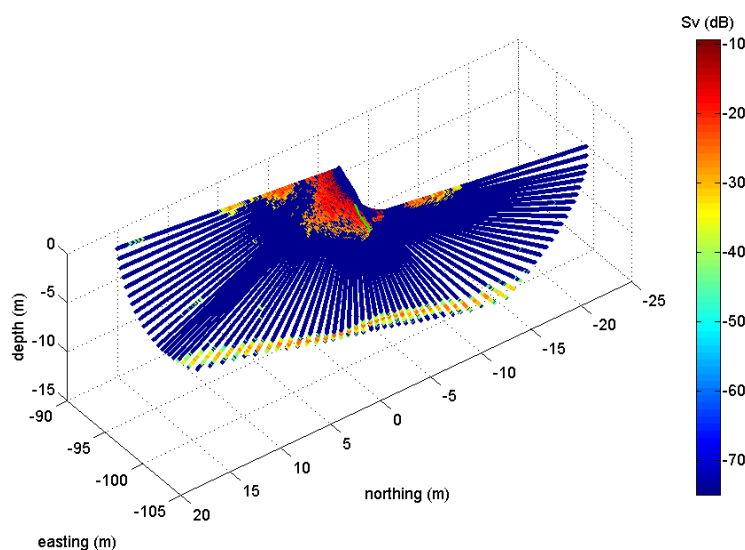


Figure 9. One-scan data geometrically corrected for sonar head orientation and boat motion.

The same data but for the whole of run 8 are presented in Figure 10. Because of the large scanning sectors, one can see that data are divided into distinct scanning sectors. The data points are much less dense than in the case of the experiment set-up 1 (Figure 5), where the sector size was only 51° . This makes the interpolation of the wake data onto the rectangular mesh less accurate. As a result the three-dimensional image of the wake in the form of contour slices is not very representative (Figure 11). Another contributing factor to this is that the wake is insonified from inside. Therefore, the large portion of the wake data in the sector above the sonar head is missing and the wake in the three-dimensional image is looking even thinner than in reality. This may be of a lesser problem for the wakes of ships larger than Ngerin, which should generate deeper and longer lasting wakes.

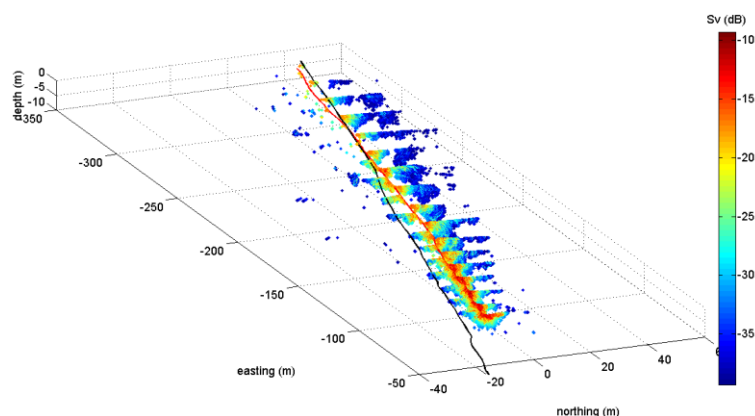


Figure 10. Sonar data bins in the fixed coordinate system. Ngerin wake during run 8. Red line – RHIB track, black line – Ngerin track.

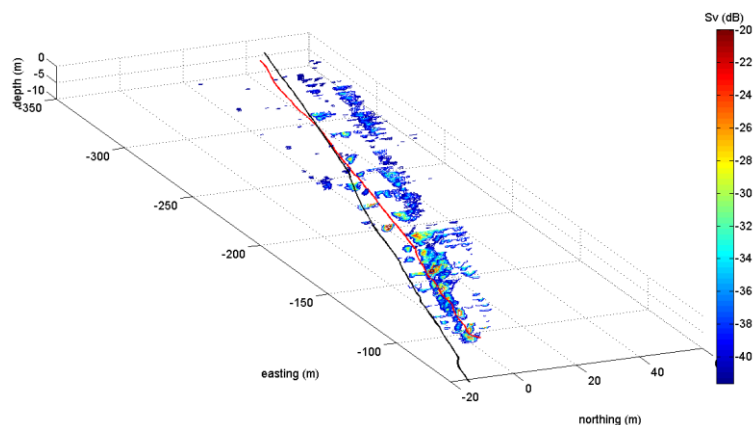


Figure 11. Contour slices of the backscattering cross-section per unit volume of Ngerin wake during run 8. Red line is RHIB track, black line is Ngerin track.

As was mentioned before, during the experiments with Ngerin wake, there was some wave action on the sea surface. Although the waves were not high from a general point of view, the wave action was significant enough to make the visual footprint of the wake disappear quicker than on the smooth surface of the Port River. This made it difficult for the RHIB coxswain to keep the boat at the centreline of the wake. It can be seen from the two plots above that RHIB's track (red line) wanders off the wake centreline.

6. Conclusion

We have considered a technique for acoustic imaging of surface ship wakes. An Imagenex high frequency profiling sonar with narrow conical beam was used for this purpose. First of all the technique provides information on the geometrical parameters of the wake. It also provides information on the backscattering cross-section per unit volume at the sonar frequency. Although the Imagenex sonar has a selectable frequency in a wide range, only one frequency can be used at a time. This makes it impossible to infer the bubble size distribution in the wake. However, even at a single frequency, the backscattering cross-section data can be useful for a ship wake model validation.

We have tested two experiment set-ups for wake insonification. In set-up 1 the wake is insonified from one side with the sonar head being outside of the wake. In the second set-up the wake is insonified from inside with sonar positioned approximately at the wake centreline. The advantage of the first set-up is that the required scanning sector is relatively narrow. This results in a relatively dense population of data points in the wake, or in other words, higher spatial resolution of the wake data. In the second set-up the scanning sector is much larger and the data points are not as dense as in set-up 1. Also a large portion of the wake above the sonar head is not insonified and is missing from the

data analysis. The disadvantage of set-up 1 is that it produces non-symmetrical images of the wake acoustic strength due to beam attenuation in the bubbly wake. This is of a lesser problem for set-up 2 provided that the sonar head is kept at the centreline of the wake.

References

1. Crisp DJ. The State-of-the-Art in Ship Detection in Synthetic Aperture Radar Imagery. Research Report Australia: Defence Science & Technology Organisation, 2004 DSTO-RR-0272.
2. Zhang X, Lewis M, Bissett WP, Johnson B, Kohler D. Optical Influence of Ship Wakes. *Appl Opt.* 2004;43(15):3122-32.
3. Bunkin AF, Klinkov VK, Lukyanchenko VA, Pershin SM. Ship wake detection by Raman lidar. *Appl Opt.* 2011;50(4):A86-A9.
4. *Physics of Sound in the Sea*: National Academies; 1949.
5. Trevor MV, Vagle S, Farmer DM. Acoustical measurements of microbubbles within ship wakes. *The Journal of the Acoustical Society of America.* 1994;95(4):1922-30.
6. Trevor MV, Vasiliev B, Vagle S. Wake acoustic measurements around a maneuvering ship. *Canadian Acoustics.* 2006;34(3):112-13. PubMed PMID: 9134598. English.
7. Weber TC, Lyons AP, Bradley DL. An estimate of the gas transfer rate from oceanic bubbles derived from multibeam sonar observations of a ship wake. *J Geophys Res.* 2005;110(C4):C04005.
8. Stanic S, Kennedy E, Brown B, Medley D, Goodman R, Caruthers J, editors. Broadband acoustic transmission measurements in surface ship wakes. *OCEANS 2007*; 2007 Sept. 29 2007-Oct. 4 2007.
9. Stanic S, Caruthers JW, Goodman RR, Kennedy E, Brown RA. Attenuation measurements across surface-ship wakes and computed bubble distributions and void fractions. *IEEE Journal of Oceanic Engineering.* 2009;34(1):83-92. PubMed PMID: 10520216. English.
10. Soloviev A, Gilman M, Young K, Brusch S, Lehner S. Sonar Measurements in Ship Wakes Simultaneous With TerraSAR-X Overpasses. *Geoscience and Remote Sensing, IEEE Transactions on.* 2010;48(2):841-51.
11. Soloviev A, Maingot C, Agor M, Nash L, Dixon K. 3D Sonar Measurements in Wakes of Ships of Opportunity. *Journal of Atmospheric & Oceanic Technology.* 2012;29(6):880-6. PubMed PMID: 76447421.
12. Imagenex, "Imagenex model 881L digital multi-frequency imaging sonar." User guide. <http://www.imagenex.com>
13. Alison Mitchell, personal communication, www.dolphinexplorer.com.au.
14. SARDI: www.sardi.sa.gov.au
15. Urick RJ. *Principles Of Underwater Sound*: McGraw-Hill Ryerson, Limited; 1983.